

## Calibration: Hardware Schemes

*John Payne  
Darrel Emerson  
Andrea Vaccari  
Last modified April 13, 1999*

---

### Revision History

*1998-07-16: First version*

*1998-11-12: Principal Milestones added, minor updates*

*1999-04-13: Major Revision (Photonic Calibration System)*

---

### Summary

In this section, hardware solutions to the problem of calibrating the MMA amplitude and phase are described. Both solutions use the blocked area in the center of the subreflector as the source of radiation from either a two-temperature load or a coherent signal source. A simple mirror mechanism is used to select between the two systems. The coherent source may be made phase stable through a round-trip measurement scheme so raising the possibility of continuous phase measurement and correction as well as providing a valuable troubleshooting tool.

**Table 3.2.1 Principal Milestones in Hardware Calibration Schemes**

	<b>Task</b>	<b>Completion Date</b>
1)	Demonstration of two temperature load. Hat Creek.	1999-October
2)	Demonstration of coherent calibration signal with round trip phase measurement.	1999-June
3)	Integration of photodiode with log-periodic antenna	1999-Dec

### 3.2.1 Introduction

The previous section describes a number of schemes for calibrating the MMA amplitude and phase. This section outlines two specific hardware calibration schemes which can help to calibrate the instrumental phase and amplitude of the MMA. Other instrumental calibration schemes, such as round-trip phase calibration for the local oscillator, and AGC/total power monitors in the I.F. chain, are described elsewhere.

The two calibration schemes outlined here are:

**Absolute temperature sensitivity calibration**, single dish mode

**Relative amplitude and phase calibration**, with an artificial coherent calibration signal suitable for interferometric calibration

### 3.2.2 Absolute Temperature Calibration

This technique is only relevant to single dish total-power observations; it has been suggested by Jack Welch and others, and is currently (July 1998) the subject of a joint MDC development between BIMA and NRAO. It gives an absolutely calibrated signal of a few K at the receiver, over the complete frequency range covered by the MMA. It has been described in [MMA Memo 225](#) by Bock, Welch, Flemming and Thornton.

The essence of this technique is that a black body radiator is placed at the center of the subreflector of each antenna, within the unused area of subreflector matching the central blockage of the antenna. In this way there is no effect on antenna sensitivity.

Within this central part of the subreflector, a plane mirror switches between two (or more) hot loads of different temperatures. The two loads have very precisely controlled and calibrated temperatures. The total power output of the receiver is sampled synchronously with the mirror switching between the two calibrated loads.

The added switched receiver noise is, to a first approximation, equal to the difference in temperature of the two hot loads, multiplied by the beam solid angle of the absorbers at the subreflector seen from the receiver feed, divided by the beam solid angle of the subreflector - assuming the receiver feed itself is matched to the angle subtended by the receiver. This ratio will be reasonably constant with frequency, but at a given frequency can be calibrated precisely by measurements of the feed antenna pattern.

For more details see the memo by Bock, Welch, Flemming and Thornton. The joint development with BIMA will show, on a timescale of a few months, how well the technique can be expected to work in practice.

### **3.2.3 Interferometric relative phase and amplitude calibration**

In the debugging stage of the MMA, there will be a need for a generic test signal that can be used to debug the entire electronic system of a given antenna or antenna pair, from front-end to correlator. When the antenna surface and pointing are sufficiently reliable, astronomical sources can be used for this purpose, but having an independent, artificially generated signal that is not dependent on antenna performance will be invaluable in checking out and maintaining the system.

If the calibration signal can be made coherent at all individual antennas, it opens up the possibility of calibrating the entire receiver system, front-ends, back-ends and correlator, amplitude and phase as a function of frequency, in a way independent of antenna tracking, pointing, or efficiency performance. The calibration system should be sufficiently stable that it can be used as a secondary calibration system, with only occasional cross-calibration with astronomical sources.

### **3.2.4 The Photonic Calibration System**

#### **3.2.4.1 Introduction**

The photonic calibration system has a broad-band, radiating antenna situated at the center of the subreflector, where no extra antenna blockage is introduced. At the feed of the broadband antenna, there is an uncooled photomixer device. A single optical fiber, carrying laser signals generated at a central laboratory or control room, feeds this photomixer. In the simplest form, the optical signal would come from two lasers, whose difference frequency corresponds to the telescope observing frequency, and which is phase-locked to the telescope frequency standard. The equipment required to do this would be nearly identical to that being developed for the photonic laser local oscillator system. Only one pair of lasers would be required for the entire array; the combined laser output would be split optically  $N$  ways (where  $N$  is the number of antennas) and routed via  $N$  independent fibers to each antenna.

In slight variants of this scheme, either a single laser signal, or the dual laser system tuned to the required mm-wave difference frequency, could be modulated. The modulation might take the form of a regular comb spectrum, simulating broadband noise. This becomes quite analogous to the pulse cal system developed for the VLBA, and could be used for checking the relative amplitude and phase response over the entire interferometric IF passband. The modulation might also be a truly random, or a pseudo-random digitally generated sequence, which would also provide a broad-band coherent test signal. This random or pseudo-random noise needs to be coherent at each antenna, so timing considerations, within a fraction of the reciprocal bandwidth, are important.

Naturally this injected signal needs to be stable, both in amplitude and phase. It may require

round-trip delay compensation of some type, and perhaps an AGC system to keep the signal amplitude constant. However, attention to the stability of this calibration signal may relax the technical requirements elsewhere in the system.

Most of the development for this coherent photonic calibration scheme is already being undertaken in the context of the photonic local oscillator development. The calibration scheme should in principle be much simpler, because several orders of magnitude lower radiated mm-wave power is required. The main additional development needed is that of the broad-band radiating antenna, to be sited at the subreflector, fed by the signal from the photomixer.

### 3.2.4.2 Requirements

The first thing we did was evaluate the minimum power required at the receiver. The total noise power ( $P_N$ ) for a receiver with system temperature ( $T_{\text{sys}}$ ) of 100 K and observation bandwidth ( $\Delta\nu$ ) of 2 GHz is given by

$$P_N = kT_{\text{sys}}\Delta\nu = 2.76 \cdot 10^{-12} \text{ W} = -85.6 \text{ dBm}$$

We want the received calibration power to be at least 1% of the total noise power:  $2.76 \cdot 10^{-14} \text{ W} = -105.6 \text{ dBm}$ .

Another requirement is that the injected signal should be linearly polarized at 45 deg with respect to the OMT or polarization grids inside the receiver so that the power is equally distributed into the two channels.

As this signal should work as a reference we need its characteristics to be as constant as possible in the whole spectral range we are going to use it: 100 GHz - 1 THz.

### 3.2.4.3 Review of antennas for radiating the signal

The best way to launch the signal towards the receiver is use an antenna placed in the blind spot of the subreflector.

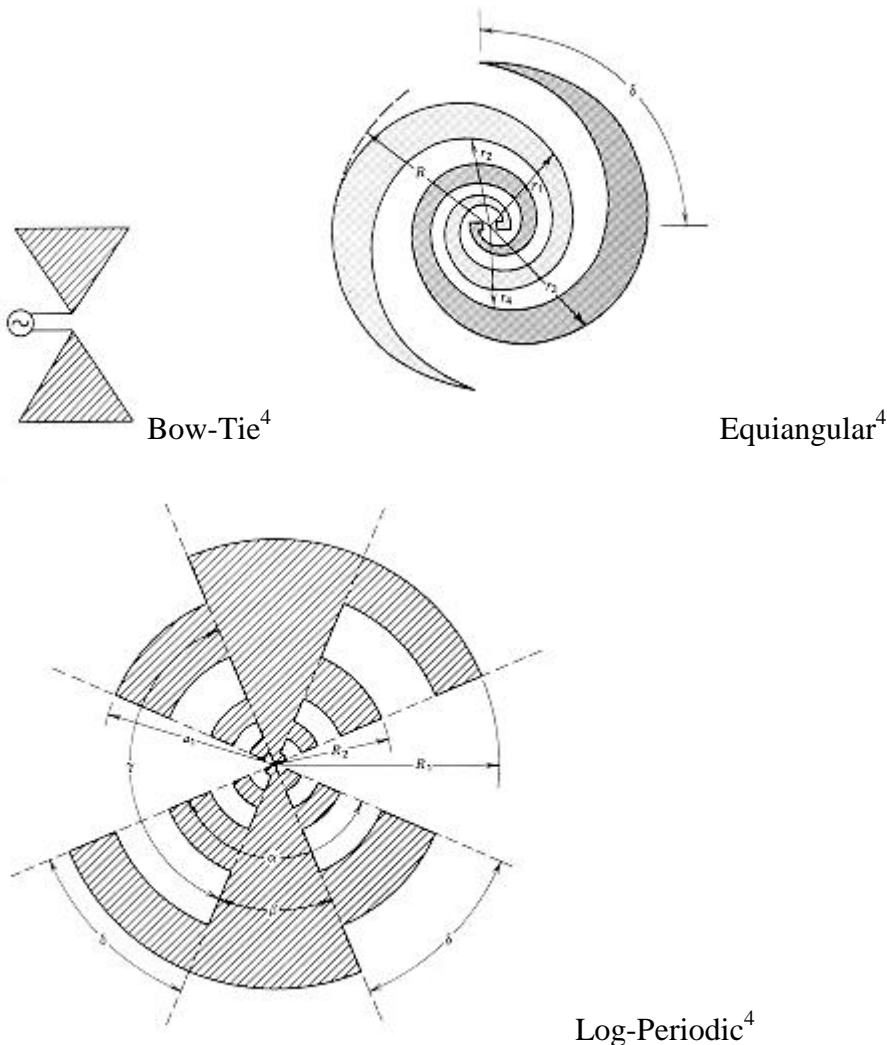
As we look at the requirements, we need an antenna with the following characteristics:

- very broad bandwidth
- linear polarization
- relatively small dimension (the transmitting system should fit in the system sketched in Fig. 4 in [MMA Memo 225: "Radiometer Calibration at the Cassegrain Secondary Mirror." & nbsp; \)](#)
- possibly high directivity (this depends on how much power we can drain from the diode that will drive the antenna)

There are few antennas that fit these requirements. We focused our attention on the *self-similar and self-complementary planar antennas*.

The self-similarity is the geometric property of invariance under a uniform expansion or reduction of size. This property implies the absence of any characteristic length scale so that the geometry is entirely defined in term of angles. This guarantees the broad bandwidth.

There are several type of self-complementary and self-similar planar antennas: Bow-Tie, Equiangular Spiral and Log-Periodic.



The Bow-Tie is the simplest, however its pattern is double-peaked off-axis<sup>5</sup> and therefore is not suitable for coupling to gaussian or other commonly encountered beams.

The Equiangular is circularly polarized<sup>1</sup>.

The beam pattern, the impedance and the rotation of the linearly polarized emitted signal of the Log-Periodic antenna are exactly periodic with the logarithm of frequency the period being given by the ratio of two successive teeth ( $R_1/R_2$ ). We decide to study with more attention this antenna because its characteristics are closer to our requirement's than the others<sup>1</sup>.

The self-complementary is the geometric property of invariance (with a rotation) under an interchange of metallized and non-metallized regions. The Booker's relation in free space for complementary antennas<sup>1</sup> states that the impedances ( $Z_1, Z_2$ ) of any pair of complementary antennas are related to the free space impedance ( $Z_0 = 120\pi \Omega$ ) by

$$Z_1 Z_2 = (Z_0/2)^2 = (189 \Omega)^2$$

As a result self-complementary antennas in free space have constant real impedance of 189  $\Omega$  at all frequency.

The purpose of our feed antenna is to couple power from a device that is much smaller than a wavelength into a wave in free space. For the frequency range we are interested in, the linear dimensions of these antennas are so small<sup>2</sup> that the best way to build them is by lithography. This manufacturing process has also the advantage to allow for an easier coupling to the emitting device since usually it is built by the same process and, by slight changes to the design, it is possible to build emitting device altogether with the antenna.

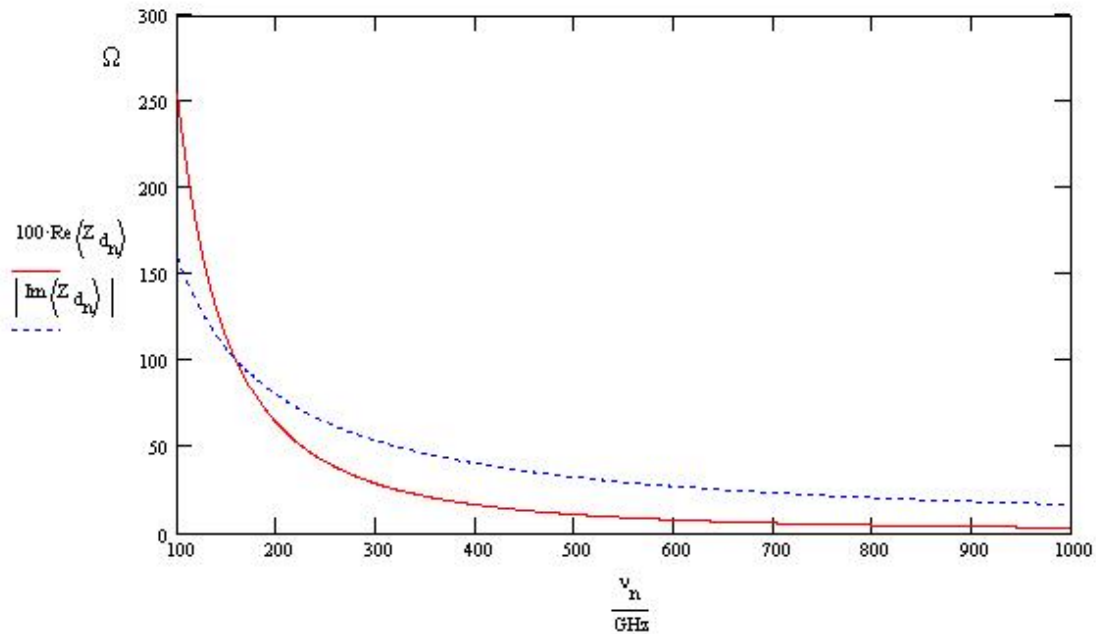
This manufacturing procedure implies a dielectric substrate over which the antenna will be deposited.

An antenna at a dielectric/air interface will preferentially couple into the dielectric substrate. In a first order the phase velocity and impedance are both reduced by<sup>3</sup>  $\epsilon_{\text{eff}} = [(\epsilon + 1)/2]^{1/2}$  it follows that for a self-complementary antenna the impedance will be  $Z = Z_0/\epsilon_{\text{eff}}^{1/2}$  (for example 74  $\Omega$  for Si o GaAs and 114  $\Omega$  for crystalline quartz)<sup>3</sup>.

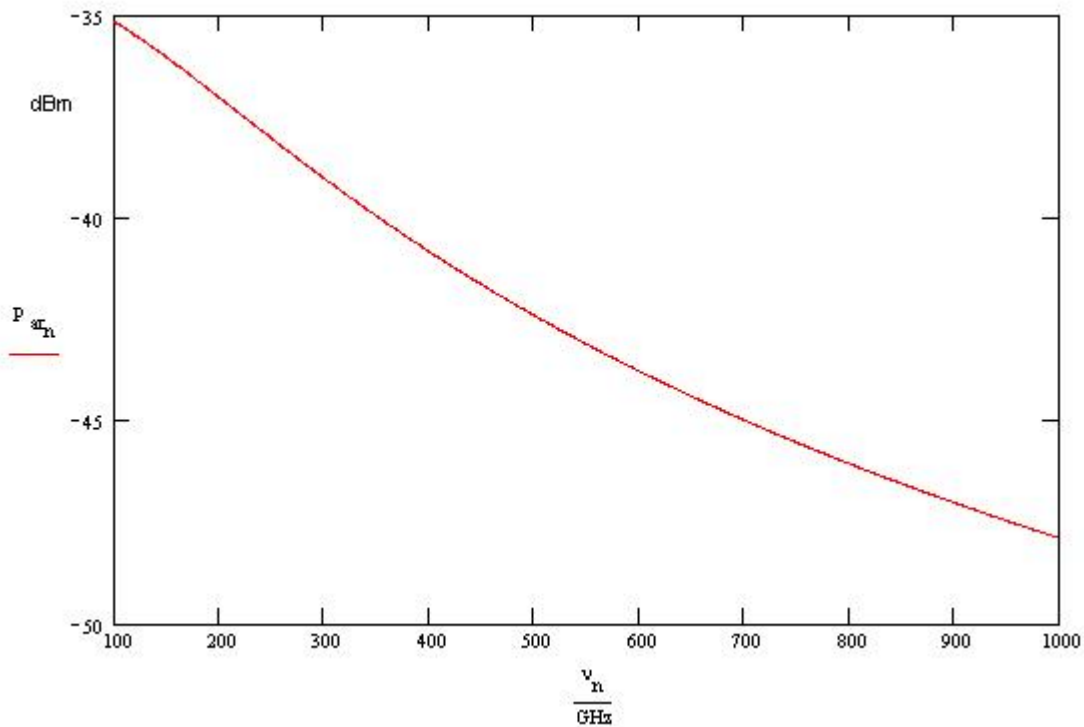
Another problem arising from the coupling in the substrate is that, in case the substrate geometry is simply a plane-parallel slab, any ray radiated from the antenna at angles exceeding the critical angle will be totally internal reflected by at the back surface of the substrate. There are two main ways to get rid of this problem. The first is to deposit the antenna on a very thin substrate (for example a free-standing membrane of silicon oxynitride and shape the holder as a horn to use all the power from the antenna). The second solution is to shape the substrate in such a way that it acts like a lens on the emitted wave. There are several shape that can be used to increase the directivity of the beam pattern: Hemisphere, Hyperhemisphere, Cartesian Oval, Dielectric Filled Parabola. We are still investigating whether and which of these shaped dielectric substrate is suitable to our purposes.

#### **3.2.4.4 Diode-Antenna matching**

These impedance values have been calculated using 10 k $\Omega$  for the diode resistance and 10<sup>-2</sup> pF for the diode capacitance and making the assumption that the diode behaves like an ideal current generator in parallel with the resistance and the capacitance. The impedance of the diode should change with the frequency approximately as in the following figure.



The real impedance has been multiplied by a factor 100. Using this evaluation for the impedance values and assuming that the antenna has a real impedance of  $74 \Omega$  we found the following results for the diode-antenna coupling.



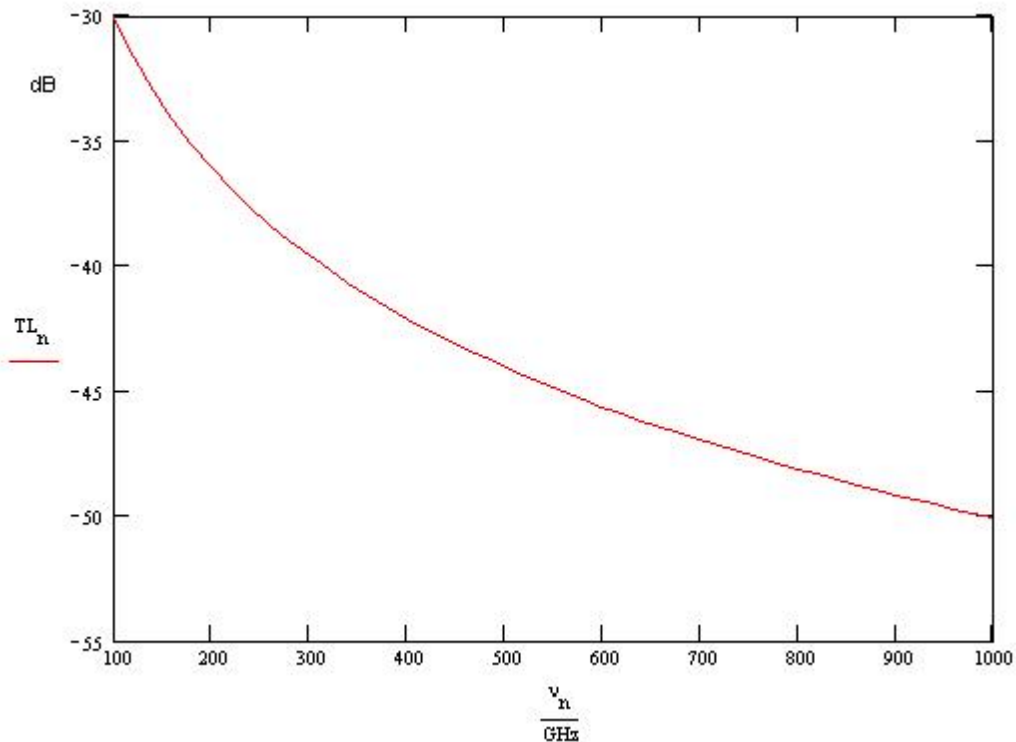
This represents the power delivered by the antenna to free space assuming that the diode is driven with a current of  $100 \mu\text{A}$ .

### 3.2.4.5 Antenna-Receiver matching

Let us consider now the efficiency of the coupling between the small antenna and the horn of the receiver. During the operation of the telescope several feed-horns will be changed to match the different frequencies so that the subreflector will always be fully illuminated, we can assume the beam pattern to be a gaussian with -11 dB point at the edge of the subreflector (3.58 deg<sup>6</sup>).

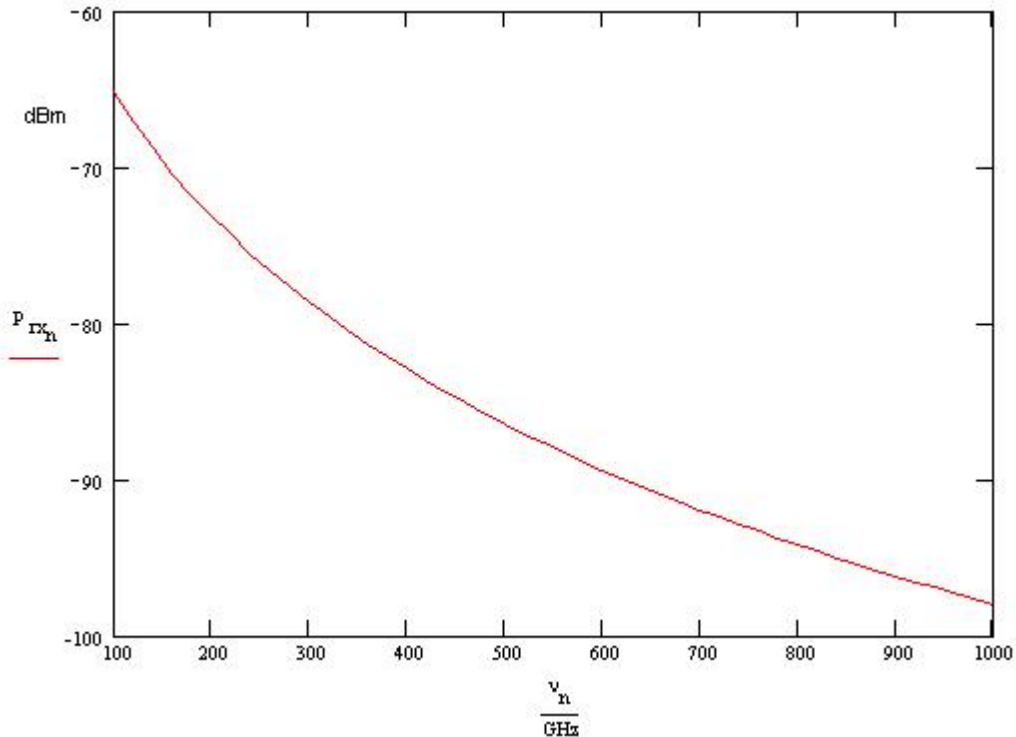
Also assume that the beam pattern of the planar antenna is a gaussian with -3 dB point at 20 deg<sup>7</sup>. As we saw we can increase the directivity by shaping the dielectric substrate.

Using these parameters we can evaluate the transmission loss of the antenna-receiver system and obtain the following result



Now if we consider the result achieved in the previous paragraph we can say that the total power available at the receiver is





The minimum power is -105.6 dBm and this result shows that with this configuration we can satisfy the power request in the whole spectral range of interest..

### 3.2.4.7 References

- [1] Victor H. Rumsey, *Frequency Independent Antennas*, Academic Press
- [2] D. Chouvaev et al. - "Normal Metal Hot-Electron Microbolometer with Andreev Mirrors for THz Space Applications" - Ninth International Symposium on Space Terahertz Technology
- [3] E.N. Grossman - "Lithographic Antennas fo Submillimeter and Infrared Frequencies" - IEEE Int. Symp. on Electromag. Compat. - 14-18 Aug. 1995, pp. 102-107
- [4] Warren L. Stutzman, Gary A. Thiele - "Antenna Theory and Design" - Wiley & Sons
- [5] G.V. Elftheriades et al - "A 20 dB Quasi-integrated Horn Antenna" - IEEE Micro. and Guided Wave Lett., Vol. 2, pp. 73-75 (1992)
- [6] MMA Memo 246: James W. Lamb - "[Optimized Optical Layout for MMA 12-m Antennas](#)"
- [7] M.A. Tarasov et al. - "Quasioptical Josephson direct detectors for mm-wave spectrum analysis" - Proc. of the Int. Conf. on mm- and submm-waves and Applications (SPIE), 10-12 Jan. 1994, pp. 220-228

### 3.2.5 Combined Calibration System

The incoherent calibration scheme described earlier switches between blackbody radiators of different temperatures using a mirror. In principle, by allowing an extra position on this mirror, the radiated calibration signal can be switched between the incoherent blackbody loads and the coherent radiator. At a later stage in the development, when the feasibility of both coherent and incoherent calibration schemes has been demonstrated, the combination of the different calibration radiators into one package will receive attention, as will studies of how to achieve the necessary amplitude and phase stability.

### 3.2.6 Work to be done

The photonic calibration builds on work already in progress in the context of the photonic local oscillator scheme, with the exception of the broadband antenna. Some simple design work is required now (e.g. exactly how much coherent power needs to be radiated from the subreflector, with what requirements on amplitude and phase stability?) but the bulk of the effort can be expected fairly late in the MMA development phase.

---

Reference:

D. Bock, J. Welch, M. Flemming and D. Thornton, [MMA Memo 225: "Radiometer Calibration at the Cassegrain Secondary Mirror."](#) (See also the [Appendix](#) below.)

---

## APPENDIX

The following figures are from the [MMA Memo 225](#) by Bock, Welch, Fleming and Thornton, "Radiometer Calibration at the Cassegrain Secondary Mirror."

**Figure 1** shows the general Cassegrain optics, which normally has a scattering cone covering the central part of the subreflector to direct unwanted rays on to cold sky. **Figure 2** shows a scattering mirror behind the subreflector, giving much the same effect.

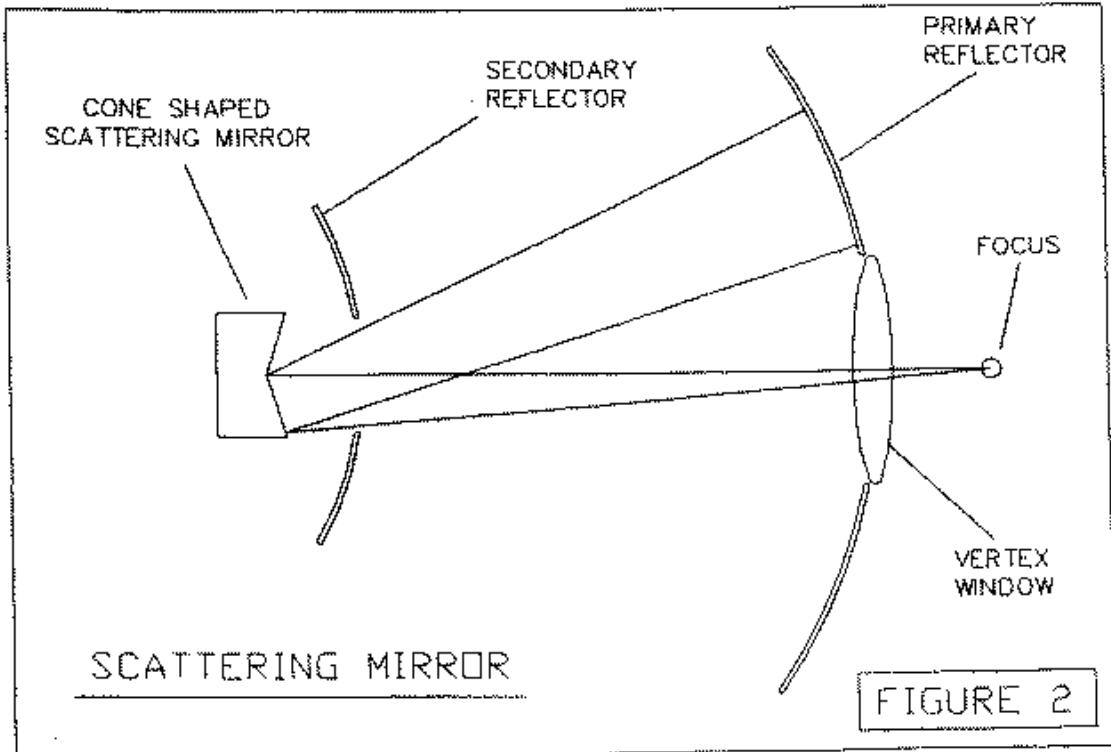
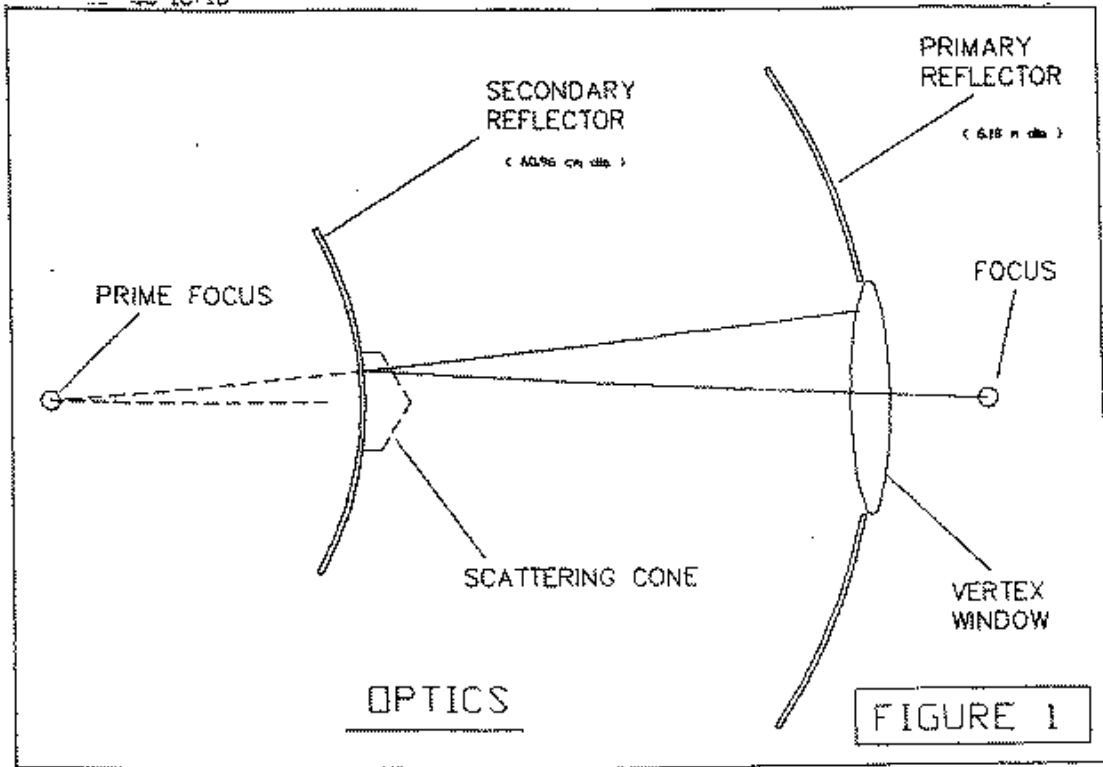


**Figure 3** shows the absorbing black body load that would be placed behind the central hole of the subreflector

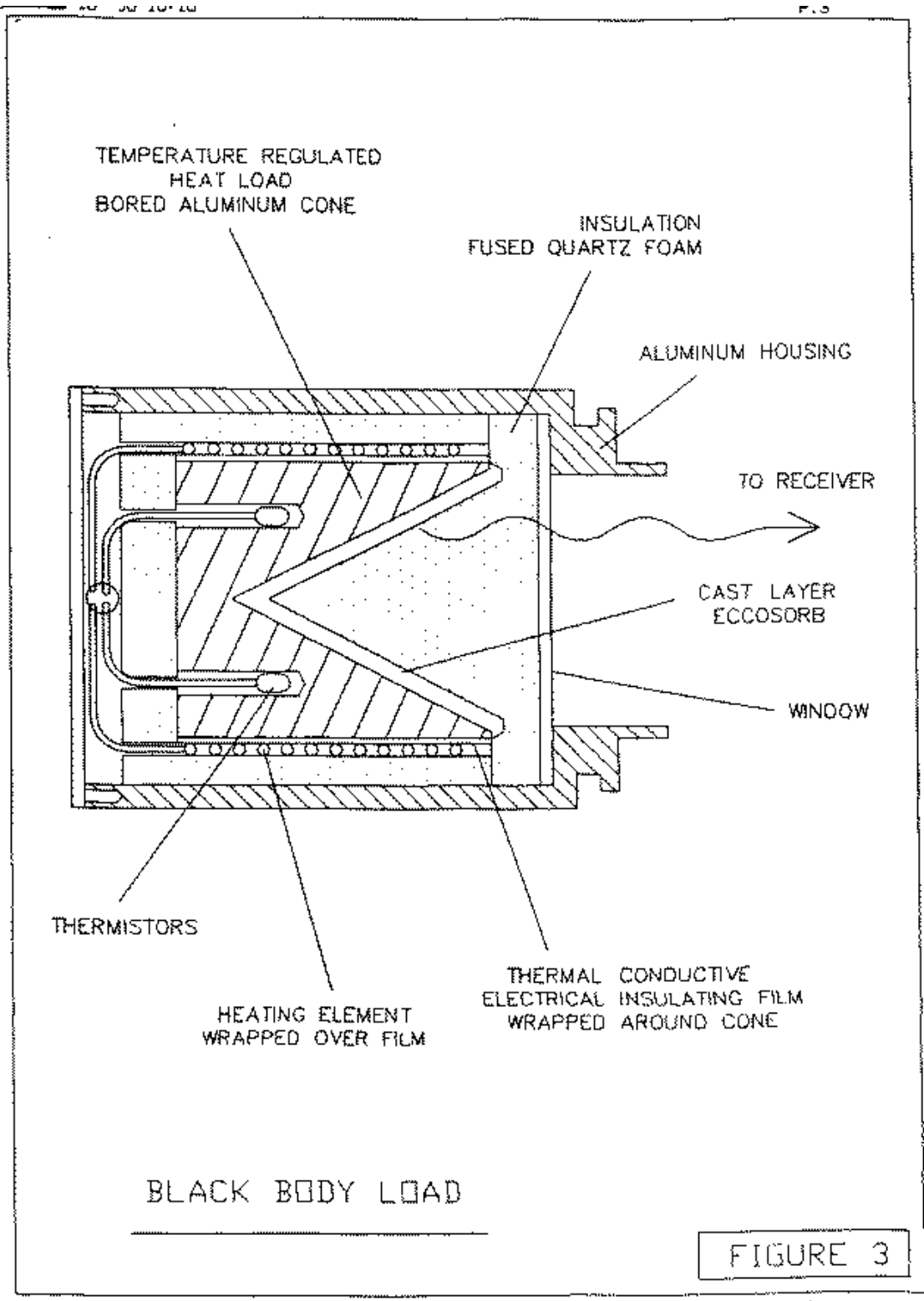


**Figure 4** shows the arrangement of a rotating 45-degree mirror which will choose between one of two hot loads, whose temperatures differ by ~100 K, and the scattering cone from which rays which eventually reach cold sky.

